geoconvention
Virtual Event September 21-23 2020
CSPG • CSEG • CWLS • GAC • MAC • IAH

Double-wavelet double-difference time-lapse waveform inversion

Xin Fu, Sergio Romahn, and Kris Innanen
University of Calgary

Summary

Time-lapse seismic data are widely used to monitor reservoir changes. And time-lapse waveform inversion is a valuable tool for seismic exploration. A popular time-lapse waveform inversion strategy is the double-difference time-lapse waveform inversion (DDWI) (inversion of the differential data starting from the reverted baseline model). It is an effective way to solve the problem that baseline and monitor inversions of time-lapse waveform inversion are easily at different convergences, and it results in coherent model error in time-lapse inversion. Nevertheless, the double-difference method (DDWI) demands an almost perfect repeatability between baseline and monitor surveys, which is the most challenging for DDWI. Specially, when sources wavelets for the two data sets are different, the results of DDWI are seriously impacted. To solve this problem, we propose a double-wavelet double-difference time-lapse waveform inversion method (DWDDWI). This works because the data difference caused by wavelet difference is eliminated. DWDDWI is developed based on the convolution relationship between the shot gather and Green's function. And its premise is that the wavelets for both baseline and monitor data sets are known. To test the feasibility of this method, a numerical example is used.

Introduction

With the increasing of exploration requirements, more powerful seismic inversion tool is needed. As a potential power to recover physical properties of subsurface rock, the full waveform inversion (FWI) is introduced to seismic exploration by Lailly and Bednar (1983) and Tarantola (1984). It is researched widely and developing fast (Virieux and Operto, 2009). Since FWI can produce inversions with a high resolution, it is helpful to estimate the parameter difference related to the subsurface property change from time-lapse data sets.

Conventionally, the baseline inversion and monitor inversion are standalone, which use the same initial model (Plessix et al., 2010). To reduce the expensive computation of performing whole FWI for twice, some researchers utilize the inverted baseline model as the initial model for monitor data inversion, this also provides a better initial model for the monitor inversion (Oldenborger et al., 2007; Miller et al., 2008; Routh and Anno, 2008; Routh et al., 2012). Unfortunately, neither the two strategies mentioned above cannot essentially remove the coherence time-lapse model error attributed to the different convergence degrees between twice inversions. To address this problem, Watanabe et al. (2004) propose the differential waveform tomography in frequency domain performed to a crosswell time-lapse data set. Onishi et al. (2009) apply a similar scheme. After that this method is developed as double-difference waveform inversion (DDWI) (Watanabe et al., 2004; Onishi et al., 2009; Zheng et al., 2011; Zhang and Huang, 2013; Routh et al., 2012; Asnaashari et al., 2011, 2012, 2013, 2015; Maharramov and Biondi, 2014; Denli and Huang, 2009; Yang et al., 2015). Successful real-data examples of DDWI are given by Yang et al. (2014, 2016) who use well-repeated ocean-bottom-cable data sets.

Nevertheless, the double-difference method (DDWI) demands a mostly perfect repeatability between the two surveys (Asnaashari et al., 2015), which is the most challenging for it. Specially, when source wavelets for baseline and monitor data sets are different, the results of DDWI are seriously impacted (Yang et al., 2015). To solve this problem, we propose a double-wavelet double-difference time-lapse waveform inversion method (DWDDWI). This works because the data difference caused by wavelet difference is eliminated. DWDDWI is developed based on the convolution relationship between the shot gather and Green's function. And its premise is that the wavelets for both baseline and monitor data sets are known. To test the feasibility of this method, a numerical example is used.

Full waveform inversion (FWI)

Full waveform inversion (FWI) as an iterative inversion method estimates subsurface parameters by matching synthetic data ($\mathbf{u_{syn}}(\mathbf{m})$), a function of model parameter $\mathbf{m}$, with observed data. The most common way to accomplish this is minimizing the L2 norm of data residual $\delta\mathbf{u}$ ($u_{syn}(m) - u_{obs}$):

$$E(m) = \frac{1}{2}\delta u^T \delta u. \tag{1}$$

Using Taylor expansion and ignoring things behind and including the second order term, we obtain linearized formula, then taking the derivative with respect to m, finally setting the derivative as zero to minimize the objective function and after easy algebraic operations, we obtain:

$$\Delta m = -H^{-1}\boldsymbol{g}, \tag{2}$$

where $\boldsymbol{H}$ and $\boldsymbol{g}$ is Hessian matrix and Jacobian matrix, respectively. To avoid the expensive computation of inversion Hessian matrix, gradient-based methods use identical matrix as an approximate substitution of $\boldsymbol{H}$, such as steepest-descent (SD) method and non-linear conjugate gradient (NCG) method (Mora, 1987; Hu et al., 2011). In this paper, we apply the SD method for FWI, which helps to converge globally (Hu et al., 2011), and the corresponding model perturbation with step length can be expressed as:

$$\Delta m = -\mu\boldsymbol{g}. \tag{3}$$

It is the negative direction of gradient and the step length μ is a constant or filter to calibrate the gradient. In this paper, we use the well-control method to calibrate the gradient, in which a segment of well log is used to figure out the step length as a factor fixing phase misfit and scaling the gradient, for details please refer to Margrave et al. (2011a) or Romahn and Innanen (2017). Also, we precondition the gradient with deconvolution imaging condition to compensate the spherical spreading of seismic wave (Margrave et al., 2011b), which can achieve the similar effect to that of approximate inverse Hessian of Shin et al. (2001) but avoid the calculation of Hessian.

Time-lapse inversion strategies

Scheme I, parallel difference method. The parallel difference method considers the baseline inversion and monitor inversion as two independent produces which use the same initial model. Then the time-lapse model comes from the difference of the twice inversions.

Scheme II, sequential difference method. It is developed from scheme I, and the only change is using the inverted baseline model as the starting model of the monitor inversion instead of the same initial model.

Scheme III, double-difference time-lapse waveform inversion (DDWI). The first inversion for the baseline data is the same as the above two schemes. But in the second inversion for the monitor data, instead of minimizing the difference between the observed and synthetic monitor data, DDWI attempts to minimize the difference between monitor and baseline data residuals. It uses a composed data as the observed data which equals to the synthetic data of the inverted baseline model plus the difference between the baseline and the monitor data. It can solve the problem that neither scheme I nor scheme II cannot essentially remove the coherence time-lapse model error attributed to the different convergence degrees between twice inversions.

Double-wavelet double-difference time-lapse waveform inversion (DWDDWI)

The composed data for the second monitor model inversion is flowing:

$$d_2 = S_{baseline} + (d_{monitor} - d_{baseline}), \tag{4}$$

where $\boldsymbol{S_{baseline}}$ is the synthetic data of the inverted baseline model, $\boldsymbol{d_{monitor}}$ is the measured monitor data, and $\boldsymbol{d_{baseline}}$ is the measured baseline data. Since a seismic shot gather can be expressed as the convolution between the source wavelet and Green' function, the above equation can be rewritten as:

$$d_2 = S_{baseline} + (W_{monitor} * G_{monitor} - W_{baseline} * G_{baseline}). \tag{5}$$

where $\boldsymbol{W_{monitor}}$ and $\boldsymbol{W_{baseline}}$ is the source wavelet for monitor and baseline shot data, respectively, $\boldsymbol{G_{monitor}}$ and $\boldsymbol{G_{baseline}}$ is Green's function for monitor and baseline shot data, respectively, and $\boldsymbol{S_{baseline}}$ is synthetic data using the baseline source wavelet. When $\boldsymbol{W_{monitor}}$ and $\boldsymbol{W_{baseline}}$ are identical, the difference is only from $\boldsymbol{G_{monitor}} - \boldsymbol{G_{baseline}}$ which is irrelevant to the wavelet. But in the case that $\boldsymbol{W_{monitor}}$ and $\boldsymbol{W_{baseline}}$ are different, the difference is from $\boldsymbol{W_{monitor}} * \boldsymbol{G_{monitor}} - \boldsymbol{W_{baseline}} * \boldsymbol{G_{baseline}}$ which is relevant both to the wavelets and Green's functions representing the property of the subsurface.

For the situation of baseline and monitor wavelets are different, we reconstruct monitor data by performing the convolution between baseline wavelet and monitor data, and reconstruct monitor data by performing the convolution between monitor wavelet and baseline data, then the new composed data becomes:

$$\begin{aligned} \mathrm{d}_2 &= \mathrm{S}'_{\mathrm{baseline}} + (\mathrm{d}'_{\mathrm{monitor}} - \mathrm{d}'_{\mathrm{baseline}}) \\ &= S'_{baseline} + (W_{baseline} * d_{monitor} - W_{monitor} * d_{baseline}), \end{aligned} \tag{6}$$

expressed with Green's function as:

$$\begin{aligned} R'_2 &= S'_{baseline} + (W_{baseline} * W_{monitor} * G_{monitor} - W_{monitor} * W_{baseline} * G_{baseline}) \\ &= \boldsymbol{S'_{baseline}} + (\boldsymbol{W} * \boldsymbol{G_{monitor}} - \boldsymbol{W} * \boldsymbol{G_{baseline}}) \end{aligned} \tag{7}$$

Where $W = W_{baseline} * W_{monitor} = W_{monitor} * W_{baseline}$ is the double wavelet which is used to generate forward modeling data $S'_{baseline}$ during the iterative wave inversion. After performing the reconstructions to baseline and monitor data sets, the new data sets are of the same wavelet W , the data difference is from $G_{monitor} - G_{baseline}$ related to the subsurface change only.

Numerical example

We do the time-lapse inversions for all the three schemes in the case that the wavelets for baseline and monitor data sets are identical. The initial model we use for the first baseline data inversion is shown in Figure 1a. And the inverted results of scheme I, II, and III are shown in Figure 1d-f. We can see that the coherence time-lapse model residual appears everywhere in the results of scheme I, II, but appears in a very small area in the result of scheme III (DDWI). In Figure 1g, we show the inverted time-lapse model of DDWI in the case of the baseline and monitor data is of 10Hz and 8Hz wavelet, respectively. Figure 1h is the inverted time-lapse model of DWDDWI in the case of the baseline and monitor data is of 10Hz and 8Hz wavelet, respectively. We can see that DDWI is seriously suffering from the unrepeatability of baseline and monitor data sets caused by wavelet difference, while DWDDWI can handle with this situation quiet well.

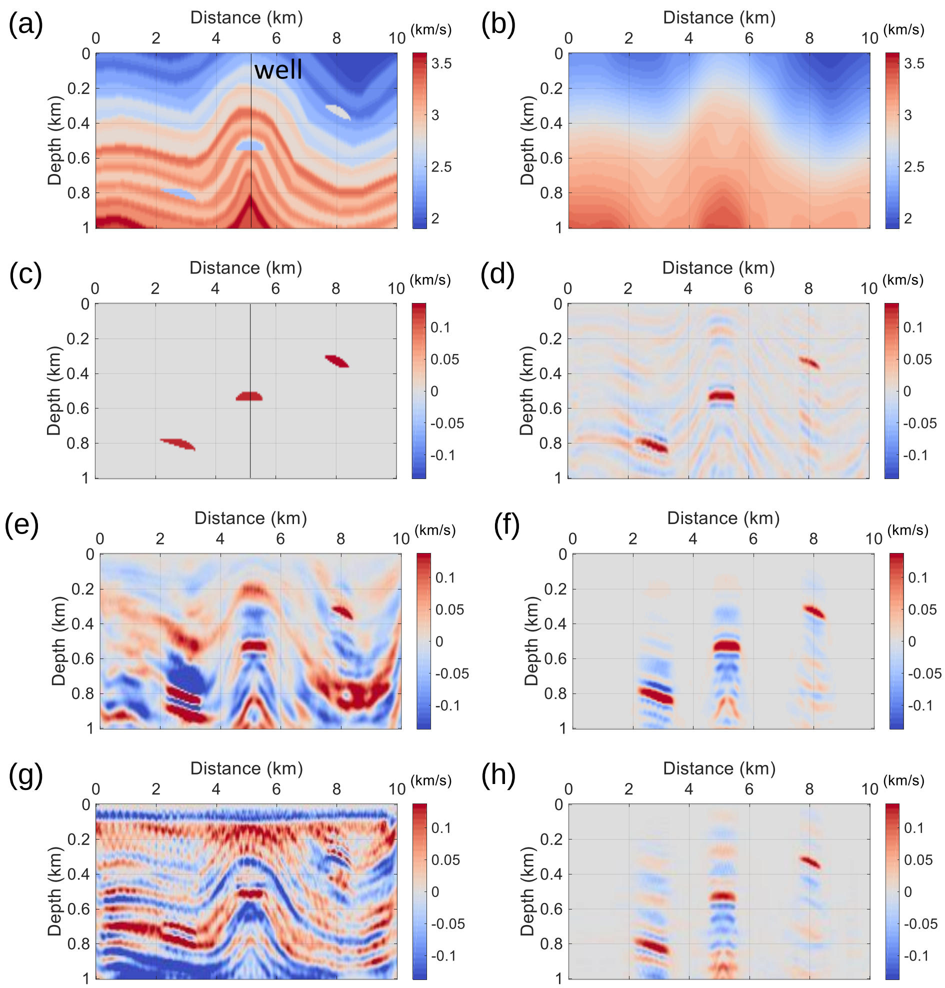

Figure 1: (a) The true baseline model. (b) The initial baseline model. (c) The true time-lapse model. (d), (e) and (f) is the inverted time-lapse model of scheme I, II, and III, respectively, in the case that the wavelets for baseline and monitor data sets are identical. (g) and (h) is the inverted time-lapse model of scheme III and DWDDWI, respectively, in the case that the wavelets for baseline and monitor data sets are different.

Conclusions

It is common view that the DDWI method has better difference recovery ability than the others. Compared with parallel difference and sequential difference time-lapse inversion strategies, DDWI is not easy to be affected by the different convergences between baseline and monitor data inversions. However, when source wavelets for baseline and monitor data sets are different, the results of DDWI are seriously impacted. but DWDDWI can handle with this situation well. DWDDWI works because the data difference caused by the wavelet difference is eliminated by the constructed common wavelet. DWDDWI is developed based on the convolution relationship between the shot gather and Green's function. And its premise is that the wavelets for both baseline and monitor data sets are known.

Acknowledgements

We thank the sponsors of CREWES for continued support. This work was funded by CREWES industrial sponsors, and NSERC (Natural Science and Engineering Research Council of Canada) through the grant CRDPJ 461179-13.

References

Asnaashari, A., Brossier, R., Garambois, S., Audebert, F., Thore, P., and Virieux, J., 2011, Sensitivity analysis of time-lapse images obtained by differential waveform inversion with respect to reference model, in SEG Technical Program Expanded Abstracts 2011, Society of Exploration Geophysicists, 2482–2486.

Asnaashari, A., Brossier, R., Garambois, S., Audebert, F., Thore, P., and Virieux, J., 2012, Time-lapse imaging using regularized fwi: a robustness study, in SEG Technical Program Expanded Abstracts 2012, Society of Exploration Geophysicists, 1–5.

Asnaashari, A., Brossier, R., Garambois, S., Audebert, F., Thore, P., and Virieux, J., 2013, Regularized seismic full waveform inversion with prior model information: Geophysics, 78, No. 2, R25–R36.

Asnaashari, A., Brossier, R., Garambois, S., Audebert, F., Thore, P., and Virieux, J., 2015, Time-lapse seismic imaging using regularized full-waveform inversion with a prior model: which strategy?: Geophysical prospecting, 63, No. 1, 78–98.

Denli, H., and Huang, L., 2009, Double-difference elastic waveform tomography in the time domain, in SEG Technical Program Expanded Abstracts 2009, Society of Exploration Geophysicists, 2302–2306.

Hu, W., Abubakar, A., Habashy, T., and Liu, J., 2011, Preconditioned non-linear conjugate gradient method for frequency domain full-waveform seismic inversion: Geophysical Prospecting, 59, No. 3, 477–491.

Lailly, P., and Bednar, J., 1983, The seismic inverse problem as a sequence of before stack migrations, in Conference on inverse scattering: theory and application, Siam Philadelphia, PA, 206–220.

Maharramov, M., and Biondi, B., 2014, Joint full-waveform inversion of time-lapse seismic data sets, in SEG Technical Program Expanded Abstracts 2014, Society of Exploration Geophysicists, 954–959.

Margrave, G., Yedlin, M., and Innanen, K., 2011a, Full waveform inversion and the inverse hessian: the 23rd Annual Research Report of the CREWES Project.

Margrave, G. F., Ferguson, R. J., and Hogan, C. M., 2011b, Full waveform inversion using wave-equation depth migration with tying to wells, in SEG Technical Program Expanded Abstracts 2011, Society of Exploration Geophysicists, 2454–2458.

Miller, C. R., Routh, P. S., Brosten, T. R., and McNamara, J. P., 2008, Application of time-lapse ert imaging to watershed characterization: Geophysics, 73, No. 3, G7–G17.

Mora, P., 1987, Nonlinear two-dimensional elastic inversion of multioffset seismic data: Geophysics, 52, No. 9, 1211–1228.

Oldenborger, G. A., Routh, P. S., and Knoll, M. D., 2007, Model reliability for 3d electrical resistivity tomography: Application of the volume of investigation index to a time-lapse monitoring experiment: Geophysics, 72, No. 4, F167–F175.

Onishi, K., Ueyama, T., Matsuoka, T., Nobuoka, D., Saito, H., Azuma, H., and Xue, Z., 2009, Application of crosswell seismic tomography using difference analysis with data normalization to monitor co2 flooding in an aquifer: International Journal of Greenhouse Gas Control, 3, No. 3, 311–321.

Plessix, R.-E., Michelet, S., Rynja, H., Kuehl, H., Perkins, C., de Maag, J., and Hatchell, P., 2010, Some 3d applications of full waveform inversion, in 72nd EAGE Conference and Exhibition-Workshops and Fieldtrips.

Romahn, S., and Innanen, K. A., 2017, Iterative modeling, migration, and inversion: Evaluating the well calibration technique to scale the gradient in the full-waveform inversion process, in SEG Technical Program Expanded Abstracts 2017, Society of Exploration Geophysicists, 1583–1587.

Routh, P., Palacharla, G., Chikichev, I., and Lazaratos, S., 2012, Full wavefield inversion of time-lapse data for improved imaging and reservoir characterization, in SEG Technical Program Expanded Abstracts 2012, Society of Exploration Geophysicists, 1–6.

Routh, P. S., and Anno, P. D., 2008, Time-lapse noise characterization by inversion, in SEG Technical Program Expanded Abstracts 2008, Society of Exploration Geophysicists, 3143–3147.

Shin, C., Jang, S., and Min, D.-J., 2001, Improved amplitude preservation for prestack depth migration by inverse scattering theory: Geophysical prospecting, 49, No. 5, 592–606.

Tarantola, A., 1984, Inversion of seismic reflection data in the acoustic approximation: Geophysics, 49, No. 8, 1259–1266.

Virieux, J., and Operto, S., 2009, An overview of full-waveform inversion in exploration geophysics: Geophysics, 74, No. 6, WCC1–WCC26.

Watanabe, T., Shimizu, S., Asakawa, E., and Matsuoka, T., 2004, Differential waveform tomography for time-lapse crosswell seismic data with application to gas hydrate production monitoring, in SEG Technical Program Expanded Abstracts 2004, Society of Exploration Geophysicists, 2323–2326.

Yang, D., Liu, F., Morton, S., Malcolm, A., and Fehler, M., 2016, Time-lapse full-waveform inversion with ocean-bottom-cable data: Application on valhall field: Geophysics, 81, No. 4, R225–R235.

Yang, D., Malcolm, A., and Fehler, M., 2014, Time-lapse full waveform inversion and uncertainty analysis with different survey geometries, in 76th EAGE Conference and Exhibition 2014.

Yang, D., Meadows, M., Inderwiesen, P., Landa, J., Malcolm, A., and Fehler, M., 2015, Double-difference waveform inversion: Feasibility and robustness study with pressure data: Geophysics, 80, No. 6, M129–M141.

Zhang, Z., and Huang, L., 2013, Double-difference elastic-waveform inversion with prior information for time-lapse monitoring: Geophysics, 78, No. 6, R259–R273.

Zheng, Y., Barton, P., and Singh, S., 2011, Strategies for elastic full waveform inversion of time-lapse ocean bottom cable (obc) seismic data, in SEG Technical Program Expanded Abstracts 2011, Society of Exploration Geophysicists, 4195–4200.